Data Engineering and Applications

Research Paper

# Koopman Neural Operator Model for Wake Interaction Prediction in Wind Farms Based on SCADA Data

**Adile Dalkıran**[1, *]

[1] Faculty of Electrical and Electronics Engineering, Bogazici University, Istanbul, 34342, Turkey
*Corresponding author: adile.da@boun.edu.tr

**Abstract.** In this research, use SCADA data to propose a Koopman neural operator model for wake interaction prediction in wind farms. Wind direction, wind speed, active power, rotor speed, pitch angle, yaw deviation, ambient temperature, generator temperature, turbine status, and downstream power-loss residuals are arranged into farm-level SCADA windows, with each turbine being considered a dynamic node. Koopman lifting is used to transform the non-linear turbine interaction into a latent evolution process with enhanced dynamical stability, and direction-conditioned wake graphs are built based on the turbine arrangement and inflow sector. Then, farm-level latent states are mapped to multi-horizon downstream power-loss, wake-intensity, and delay predictions using a compact neural operator. Improved power-loss RMSE, wake-intensity F1, delay-error control, cross-sector transfer, and online inference latency are demonstrated using simulated trials of an irregular 42-turbine wind farm. The model is neither a direct flow-measurement or automatic-control system, but rather a SCADA-based monitoring layer for wind-farm operators.

**Keywords:** *Wind Farm SCADA, Wake Interaction, Koopman Neural Operator, Power Loss Prediction, Wind Energy Forecasting*

Received on 26 November 2021, Accepted on 09 February 2022, Published on 18 February 2022



## Introduction

A large wind farm should be viewed as a combined-energy system rather than a group of standalone turbines. When an upstream turbine extracts kinetic energy from the incoming flow, the downstream flow is slower and more turbulent; thus, the downstream power is reduced, load fluctuations occur, and the response delay is extended. Wind Direction, Turbine Spacing, Topography, Yaw Misalignment, Pitch Control and Atmospheric Conditions all affect wake interaction. Supervisory control and data acquisition records provide continuous operating data for the above processes, including wind speed, active power, rotor speed, nacelle direction, pitch angle, generator temperature and status, etc., for each turbine. Wake-modeling research has shown that a single free-stream wind speed can no longer accurately explain the power loss of downstream turbines [1], and wind farm operation studies have determined that SCADA-based monitoring is suitable for performance analysis and fault detection [2]. Thus, for wake interference prediction, both farm-scale spatial cooperation and turbine-level temporal data are required.

Wake interaction is non-linear, delayed and anisotropic. Waves and local turbulence are caused by changes in the wind field; therefore, an upstream change in operation will not immediately affect a downstream turbine. A small change in the angle of the inflow can cause a strong wake connection to disappear or show a different turbine row. Liu et al. [3] have improved short-term wind power forecasting using data-driven methods, and Khodayar and Wang [4] have developed a graph-based spatiotemporal learning model for wind farm topology and inter-turbine dependencies. Most forecasting models are still treating SCADA sequences as general multivariate time series. The above models can predict the farm power, but they cannot determine which upstream turbine affects which downstream turbine, how long the wake delay is, or whether a reported loss is due to local turbine conditions or wake interaction.

Koopman Learning can be used to address the above problem. Assume that the original nonlinear SCADA variables change linearly; otherwise, map the turbine states to a latent observable space and use a linear operator for the approximation of the primary evolution. Neural operator learning can then learn mappings from functional inputs to dynamic outputs over multiple farm operating windows. Neural operator techniques have done well in learning complex physical mappings [5], and Koopman-based machine learning has also been used for nonlinear dynamic systems [6]. Wake processes of wind farms have physical structures, but these structures are difficult to capture with a single analytical wake model under all terrain, inflow and control conditions. Koopman neural operators can thus combine interpretable latent dynamics with data-driven flexibility.

This is how the remainder of the paper is structured. Reviews in Section 2 Koopman operator learning, neural operator forecasting, wake interaction prediction, and wind farm monitoring powered by SCADA. The suggested model, which comprises neural operator mapping, Koopman latent evolution, wake coupling graph design, SCADA feature tensor generation, and prediction target, is presented in Section 3. The experimental setup, wake-state distribution, multi-horizon prediction outcomes, delay error, ablation trials, cross-farm transfer, and online deployment analysis are all included in Section 4. The study findings are presented in Section 5, along with future directions for field-level adaptive calibration, turbine-load coupling, and physics-informed limitations.

## Related Work

### SCADA-Driven Wind Farm Monitoring and Wake Prediction

By continuously gathering environmental and turbine data, SCADA data provide an accessible source for analyzing a wind farm's operational circumstances. SCADA records can display seasonal operation, shutdown events, curtailment, turbine control status, and farm-level production changes in contrast to short field campaigns that employ Lidar or met-mast data. SCADA signals have been exploited by Leahy et al. [7] to detect anomalous behavior and performance declines. Because the power loss downstream is correlated with the operation, wind direction, and turbine layout upstream, Shaler et al. [8] have also demonstrated that SCADA data are appropriate for wake prediction. However, control operations may have an impact on time-averaged and noisy SCADA data. Thus, curtailment, sensor drift, yaw misalignment, ice, local turbine problems, and actual wake contact should all be distinguished by a wake predictor.

Historically, wake interaction models have been classified into three categories: engineering wake models, computational fluid dynamics (CFD)-based models, and analytical-assumption-based models. Although these methods have strong physical interpretability, they are not appropriate for all types of topography, inflow directions, and turbine configurations. Data-driven approaches should not be regarded as black-box power-curve models, even though they can learn site-specific behavior from operational experience. Time dependency and uncertainty have recently been incorporated into wind power forecasting studies [9]. Turbine spacing and wind-direction impacts have been modeled using graph-learning techniques [10]. In row-like or irregular turbine layouts, wake connections are not symmetric; in a given wind sector, an upstream turbine may have an impact on a downstream turbine, but the opposite influence should be minimal. As a result, a directed wake graph rather than a fully linked farm representation is used in this work.

The same working logic is used in this study. A turbine-level temporal tensor is constructed using SCADA variables, and dynamic wake graphs are produced based on wind direction and turbine coordinates. Additionally, the model will forecast the overall farm power as well as the wake-delay response, interaction intensity, and other aspects of the downstream power loss. Differentiate between these causes because wind-farm operators need to know if a power loss is caused by wake effects, wind variations, turbine curtailment, or other regional issues. Yaw optimization, turbine grouping, power-loss attribution, and aberrant wake detection may all be supported by a wake-aware prediction model.

### Koopman Operator Learning and Neural Operator Forecasting

Nonlinear dynamical systems are represented by Koopman operators as linear progression in a larger observable space. By making many nonlinear processes easier to anticipate and comprehend using learnt latent observables, this will benefit the engineering system. Koopman learning techniques have recently estimated latent evolution from data using autoencoders, recurrent networks, and dynamic mode decomposition [11]. Latent linear evolutions can be used to illustrate recurring dynamic patterns of wake delay, wake recovery, and ramp response in wind-energy applications [12]. For turbine spatial connections that vary with wind direction, a single Koopman model might not be appropriate. Inform the operator of the turbine's working condition as well as the farm layout.

The concept is expanded upon by neural operators, which may learn mappings from input functions to output functions in addition to fixed-dimension vectors. In recent years, fluid dynamics and spatiotemporal prediction have been studied using Fourier Neural Operators and other operator-learning techniques [13]. For the purpose of predicting wake interactions, a neural operator can learn how to translate a farm-level SCADA window to a downstream wake-loss field across many horizons. Other techniques for simulating spatial dependency and delayed reactions include Graph Neural Networks and Temporal Attention Models [14]. Large neural operators, however, are too heavy for online farm monitoring and regular SCADA updates. As a result, the suggested model is a comparatively straightforward Koopman neural operator that preserves the interpretability of latent evolution while limiting mapping complexity.

The model's design will also satisfy the needs of online prediction. Obtain fresh SCADA windows at the wind farm's control center on a regular basis and demand reliable projections for every wind-direction sector. For operational decision support, a model that works well offline but becomes unstable under infrequent influx circumstances is not appropriate. Cross-site transferability, uncertainty estimates, and model resilience are all studied in renewable energy forecasting [15]. Both turbine load and power production are affected by wake-induced events including yaw misalignment and derating, therefore the projections must also be realistic and safe [16]. Therefore, instead of just concentrating on average error, the suggested technique reports multi-horizon prediction, wake-delay interpretation, module contribution and deployment latency, etc.

## Proposed Model

### SCADA Feature Tensor and Wake Coupling Graph

The farm SCADA records are first organized into turbine-level state vectors. For turbine i at time t, the operating vector includes wind speed, active power, rotor speed, pitch angle, yaw deviation, nacelle direction, ambient temperature, generator temperature, and turbine status flags. These variables jointly describe local turbine behavior, environmental condition, and possible operational constraints.

$$x_i^t = [v_i^t, p_i^t, \omega_i^t, \theta_i^t, \psi_i^t, \eta_i^t, T_i^t, s_i^t] \quad \text{Eq.(1)}$$

Both the controlled-turbine state and the environment are preserved in this vector. Power is insufficient because wake contact, curtailment, or changes in turbine status may result in a decrease in downstream power.

$$X^t = [x_1^t, x_2^t, \dots, x_N^t] \quad \text{Eq.(2)}$$

All turbine vectors are stacked at the same SCADA time step to create the farm-level state. This approach allows the model to compare upstream and downstream turbines within the same operating window.

$$a_{ij}^t = \exp\left(-\frac{d_{ij}}{\sigma_d}\right)\max\left(0, \cos\left(\gamma^t - \gamma_{ij}\right)\right) \quad \text{Eq.(3)}$$

Wind direction and turbine spacing determine the wake adjacency coefficient. A turbine pair receives a high graph weight only when turbine j is located in a plausible downstream wake sector of turbine i, based on relative bearing, distance, and current inflow direction. The graph is therefore dynamic rather than fixed, because the upstream source and downstream receiver can change when the wind sector changes.

$$G^t = (V, A^t), A^t = \left[a_{ij}^t\right] \quad \text{Eq.(4)}$$

A wake graph changes when the wind direction changes. The construction of the SCADA feature tensor and wake coupling graph, as well as the conversion of raw turbine records, layout coordinates, wind-sector alignment, and status filtering into a directed wake graph, are depicted in Figure 1.

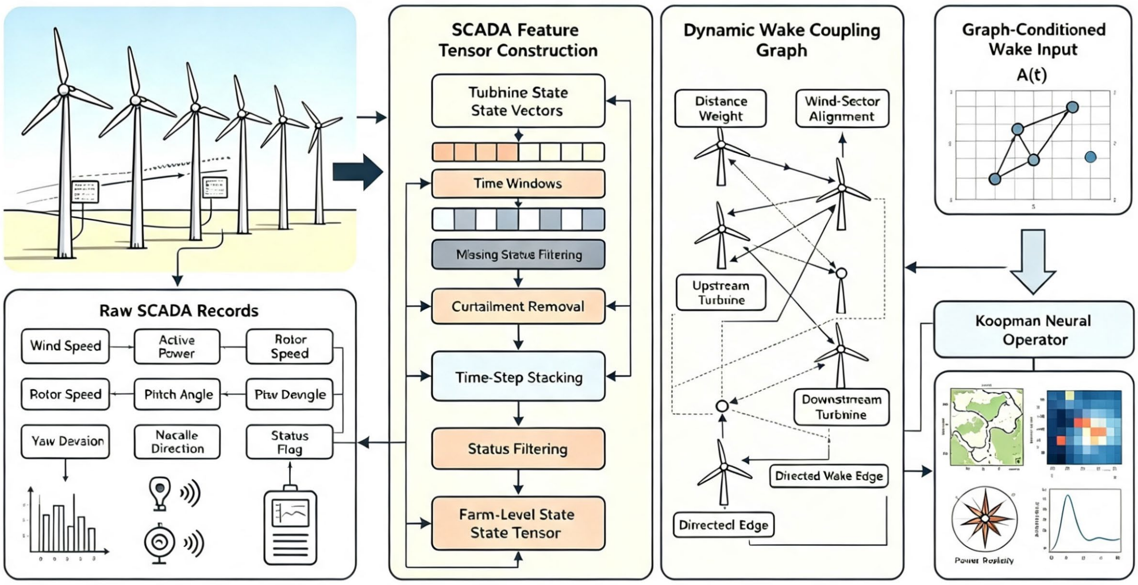


Figure 1. SCADA feature tensor and wake coupling graph.

**Koopman Neural Operator Evolution**

After creating the wake graph, transfer the turbine states to the latent observable space. The nonlinear wake interaction is expressed through latent evolution in a rather regular way by introducing a lifting function. Both local turbine behavior and upstream influence may be included in the latent vector as the lifted state comprises a turbine's operational characteristics and graph-related wake information.

$$z_i^t = \Phi_\theta(x_i^t, g_i^t) \qquad \text{Eq.(5)}$$

The lifted state combines turbine operating features and graph-related wake context. This makes the latent vector sensitive to both local turbine behavior and upstream influence.

$$Z^t = [z_1^t, z_2^t, \dots, z_N^t] \qquad \text{Eq.(6)}$$

A graph-conditioned Koopman transition propagates the whole latent farm state throughout time. This method predicts the latent evolution and uses the dynamic wake graph to identify the intensity and direction of its transition rather than directly modeling all the nonlinear interactions in the original SCADA space. Adapt the upstream-downstream propagation in response to a shift in wind direction.

$$\tilde{Z}^{t+1} = K_\theta(A^t)Z^t \qquad \text{Eq.(7)}$$

The transition matrix is conditioned on the dynamic wake graph. When the wind direction changes, the operator changes the strength and direction of inter-turbine propagation.

$$\tilde{Z}^{t+\tau} = K_\theta(A^{t+\tau-1}) \cdots K_\theta(A^t)Z^t \qquad \text{Eq.(8)}$$

The multi-step latent prediction supports wake-delay modeling because downstream influence may appear several SCADA intervals after upstream operation changes.

$$\mathcal{O}_\theta(F)(i,\tau) = \int_\Omega \kappa_\theta(i,j,\tau)F(j)dj \qquad \text{Eq.(9)}$$

The neural operator maps farm-level latent functions to turbine-horizon responses. The kernel captures how upstream states are transformed into downstream wake effects.

$$\hat{y}_i^{t+\tau} = D_\theta\left(\mathcal{O}_\theta(\tilde{Z}^{t+\tau})_i\right) \qquad \text{Eq.(10)}$$

The anticipated downstream power loss, wake influence intensity, and effective delay are all output by the decoder. The underlying structure depicted in Figure 2 includes Koopman lifting, graph-conditioned latent propagation, operator mapping, and multi-horizon wake prediction.

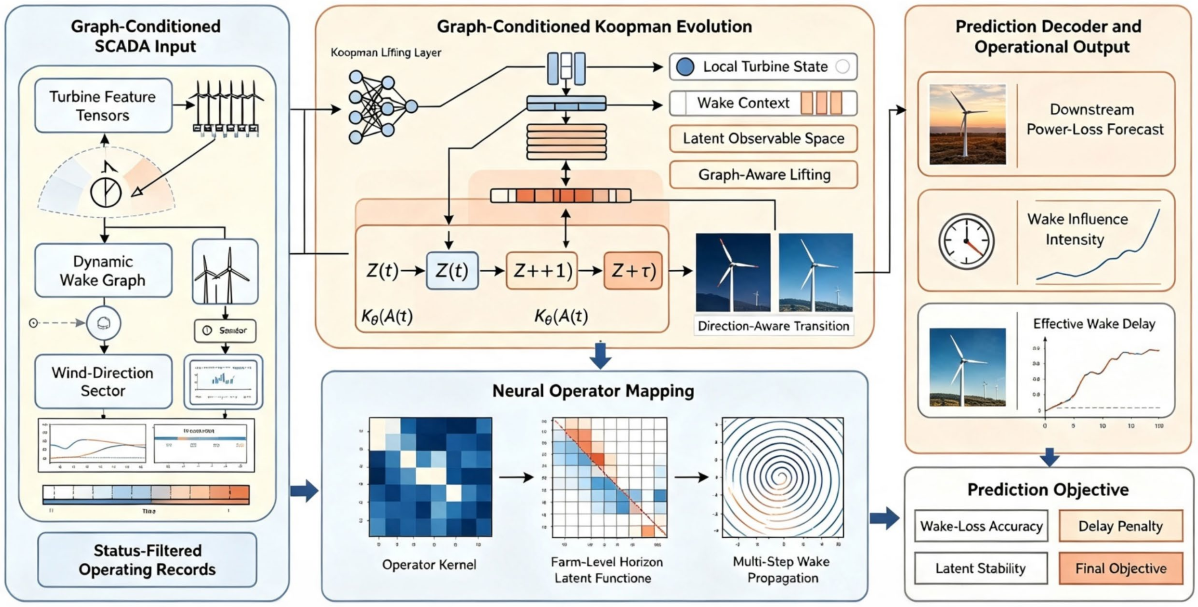


**Figure 2.** Koopman neural operator evolution structure.

**Wake Loss, Delay Penalty, and Prediction Output**

Turbine-level power-loss residual, wake-interaction probability, wake-intensity category, and effective delay are the output goals. After obtaining a wake-related loss signal by comparing the measure power with a reference non-wake power curve, unavailable status records, shutdown times, and clear curtailment intervals are eliminated prior to supervision.

$$\ell_i^t = \max\left(0, p_{i,\mathrm{ref}}^t - p_i^t\right) \qquad \text{Eq.(11)}$$

This loss term is used only after removing unavailable status records and obvious curtailment intervals. It gives the model a supervised signal for downstream wake influence.

$$L_p = \frac{1}{NT}\sum_{i,t}\left(\ell_i^t - \hat{\ell}_i^t\right)^2 \qquad \text{Eq.(12)}$$

The power-loss prediction loss trains the model to estimate the magnitude of wake-related reduction.

$$L_d = \frac{1}{NT}\sum_{i,t}\left|\Delta_i^t - \hat{\Delta}_i^t\right| \qquad \text{Eq.(13)}$$

The delay penalty modifies the anticipated wake arrival time. If a model forecasts the downstream reaction too early, too late, or allocates it to the incorrect upstream turbine, it is still operationally faulty even if its average power error is appropriate. To avoid unduly significant latent trajectory variations brought on by tiny SCADA changes, a Koopman stability element is introduced.

To guarantee the stability of Koopman evolution and avoid a significant divergence of the latent trajectory brought on by little SCADA changes, a stability term has been introduced.

$$L = L_p + \lambda_d L_d + \lambda_s L_s \qquad \text{Eq.(14)}$$

Lastly, maximize the trade-off between latent stability, delay estimation, and wake-loss accuracy. For operational analysis, the trained model produces the farm-level interaction map, downstream power loss forecast, and turbine-level wake intensity.

## Experimental Results and Discussion

### Dataset Setting and Wake-State Distribution

The experimental dataset generates a simulated wind-farm SCADA prediction problem. It has an irregular onshore arrangement of 42 turbines, a 10-minute SCADA interval, and records turbine coordinates, wind direction, wind speed, active power, rotor speed, pitch angle, yaw deviation, generator temperature and status flags. Normal inflow, partial wake, severe wake, curtailment-like operation, direction transition and turbine-status disturbance are all included in the simulation. Wind power forecasting studies show that the evaluation window should cover changes in wind and turbine conditions [17], and wind-farm SCADA analytics require filtering of operational data before performance modelling [18]. Wake labels are generated from upstream-downstream power-loss consistency after suspicious curtailment intervals have been identified and shutdown records deleted. The split is 70% training days, 10% validation days, 20% test days, and the reserved wind-direction sectors are for transfer evaluation.

The wake-state distribution and dataset composition are as follows: Figure 3. The proportions of normal, weak-wake, medium-wake, and strong-wake samples are shown in Figure 3(a), and severe wake cases are relatively infrequent compared to normal production intervals. Wind-speed bins are shown in Figure 3(b); most samples fall in the range of 6-11 m/s, and wake-induced power loss is more pronounced here. Wind-direction sectors in Figure 3(c) show that the interaction graph is not fixed, and turbine-row categories in Figure 3(d) distinguish between upstream, middle-row, downstream, and edge turbines. Together, the above subfigures show that wake prediction is not a simple farm-power forecasting problem; therefore, the model needs to know the turbine's position, active inflow sector, and physically plausible downstream response.

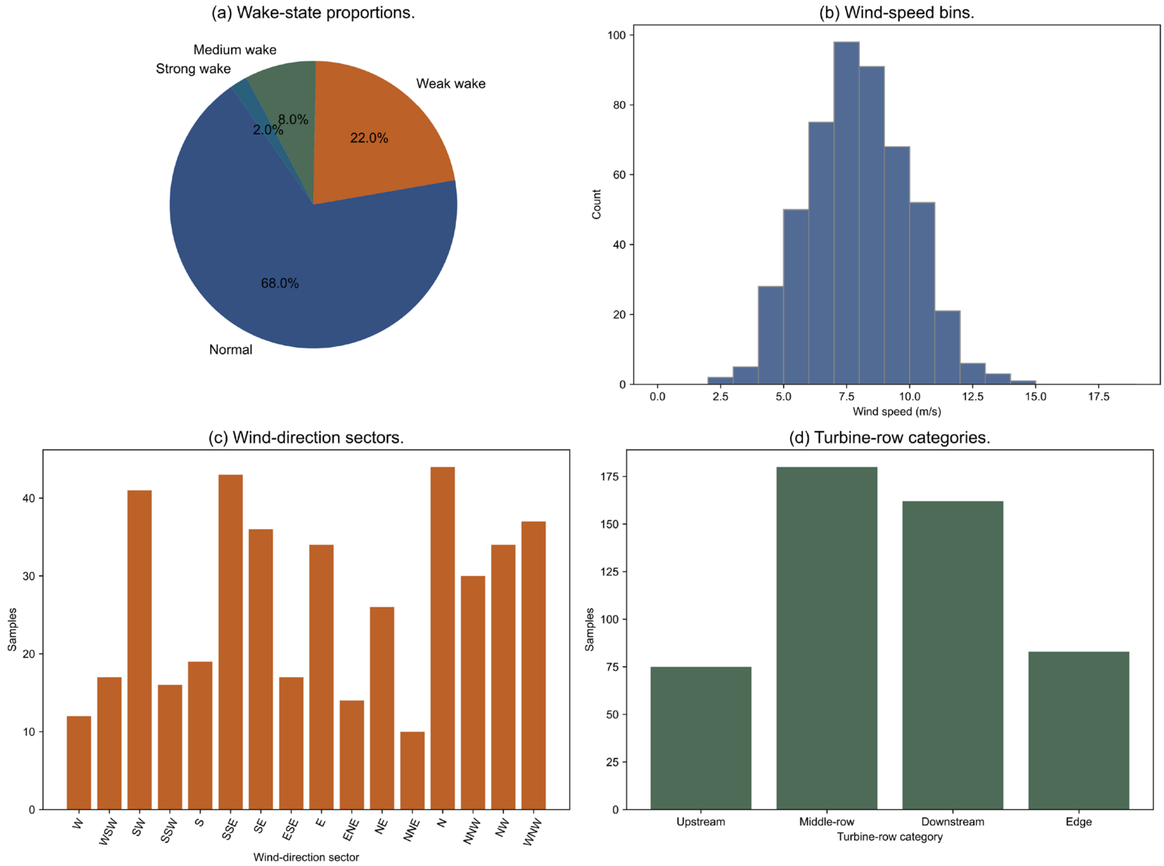


**Figure 3.** Dataset composition and wake-state distribution. (a) Wake-state proportions. (b) Wind-speed bins. (c) Wind-direction sectors. (d) Turbine-row categories.

Wake interaction is not evenly distributed throughout the farm. Edge turbines generally have a cleaner inflow and are situated upstream of the middle-row turbines, which may be sources or receivers depending on the wind direction. Downstream turbines have a higher power-loss variance, but not all power reductions are due to wake interaction. Pitch control, temperature limitation, curtailment and turbine status change will also reduce

https://doi.org/10.64972/dea.2022.v1i1.3985d:57-68

power. Therefore, the proposed model does not treat every low-power interval as a wake-up event but uses status filtering and graph alignment.

Another unbalanced prediction situation is the wake-state distribution. Strong-wake and rapid-direction-transition events are very rare, and the majority of SCADA intervals are in the typical or weak-wake condition. A model that is only optimized for the mean power error would not be able to handle uncommon but significant farm-level situations. Power-loss RMSE, wake-intensity F1, delay error, sector-transfer performance, and inference latency will thus be used in the assessment. Because the operator needs not only the anticipated value but also an explanation of the wake interaction's origin and if the forecast can be reached before the next SCADA update, this combination is more suited for operation. Although the strong wake and direction-transition windows combined make up a far lower percentage of the data in the simulated records than they do in the typical production windows, these windows are more important for operational judgment. By projecting a near-normal condition most of the time, a conservative model can achieve a low average error, but it will miss times when the downstream turbines need to be attended to. As a result, merely a mediocre level of smoothness will not be awarded. Assess if the calculation speed satisfies the need for numerous SCADA updates, whether a rare strong-wake event has happened, and how well the expected delay matches the actual response. As a result, the experiment is more challenging and has less to do with farm monitoring.

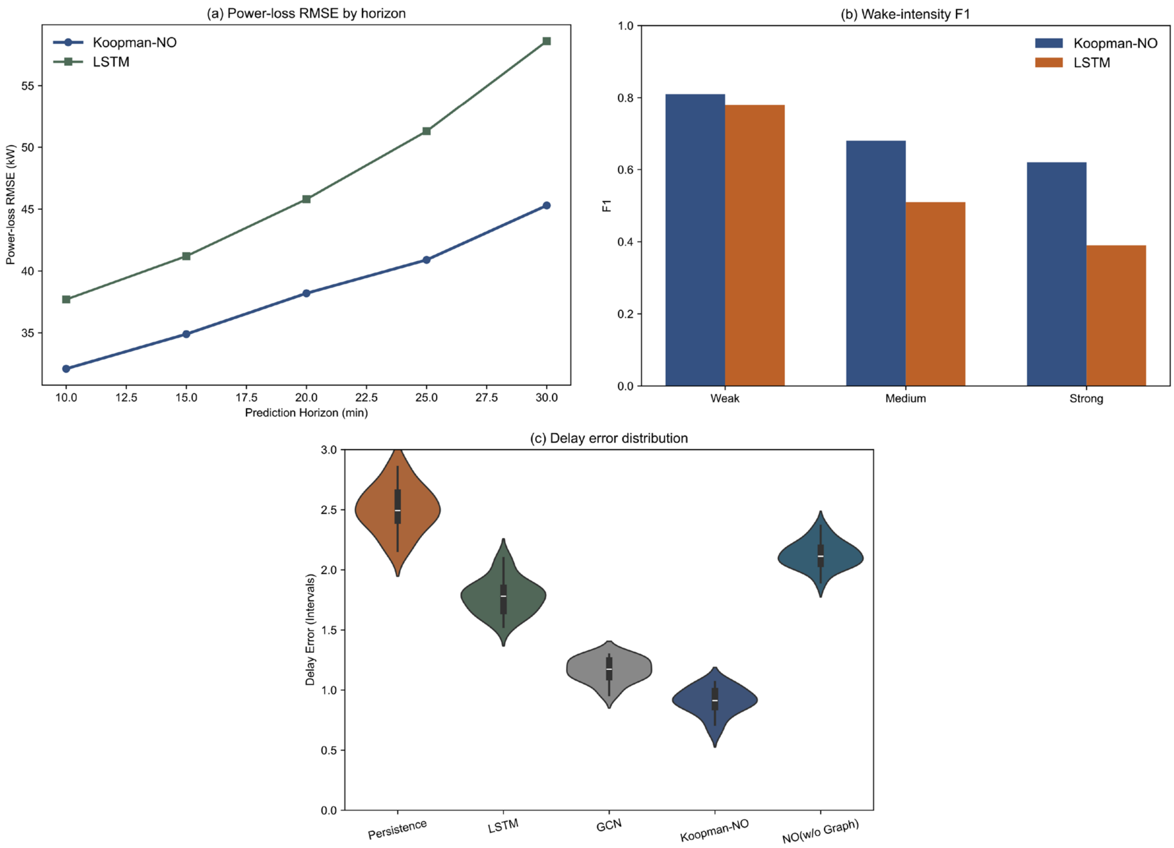


**Figure 4.** Prediction performance and delay evaluation. (a) Power-loss RMSE by horizon. (b) Wake-intensity F1. (c) Delay error.

### Prediction Performance and Wake-Delay Error Analysis

Persistence prediction, random forest, XGBoost, LSTM, temporal convolution network, graph convolutional network, graph recurrent network, vanilla neural operator, and Koopman autoencoder without wake graph conditioning are used as baselines. The proposed Koopman neural operator is evaluated at 10-, 20-, and 30-minute horizons. Lim et al. [19] proposed multi-horizon assessment for time-series forecasting, and graph-based wind-farm prediction shows that turbine-relationship modeling improves farm-level prediction [20]. The proposed model performs best at the 20-minute horizon and achieves the lowest downstream power-loss RMSE across all horizons. This is meaningful because wake effects often appear after transport delay rather than immediately after upstream power fluctuation. LSTM can learn temporal correlation but cannot identify the source turbine directly, while graph models need wind-direction-conditioned edges to represent changing wake paths.

The initial forecast result is shown in Figure 4. Power-loss RMSE by prediction horizon in Figure 4(a) shows that the proposed model remains stable at both 10-minute and 30-minute horizons. Wake-intensity F1 for weak, medium, and strong wake categories is shown in Figure 4(b), where upstream-downstream graph alignment improves strong-wake identification. Figure 4(c) shows that the average delay error is reduced from 1.82 SCADA intervals for LSTM to 0.91 intervals for the proposed method. The three panels jointly evaluate magnitude accuracy, wake-class recognition, and timing reliability. A model can be close to measured power but still be operationally invalid if it predicts the wrong arrival time or attributes the wake to the wrong upstream turbine.

A detailed error analysis of representative operational cases is displayed in Figure 5. A stable wind-sector case is shown in Figure 5(a), where the proposed model maintains a cleaner downstream wake-intensity map while most baselines also match power reasonably well. A wind-direction transition case is shown in Figure 5(b); the static-graph baseline still attributes the loss to the previous upstream turbine, whereas the proposed model updates the wake adjacency. Strong-wake underestimation cases are shown in Figure 5(c), and the model remains uncertain when SCADA status labels do not fully separate turbine derating or curtailment from wake effects. Koopman learning experiments improve nonlinear dynamic prediction through latent stability [21], and neural-operator studies show that learned mappings can generalize to function inputs but still need relevant physical conditioning [22].

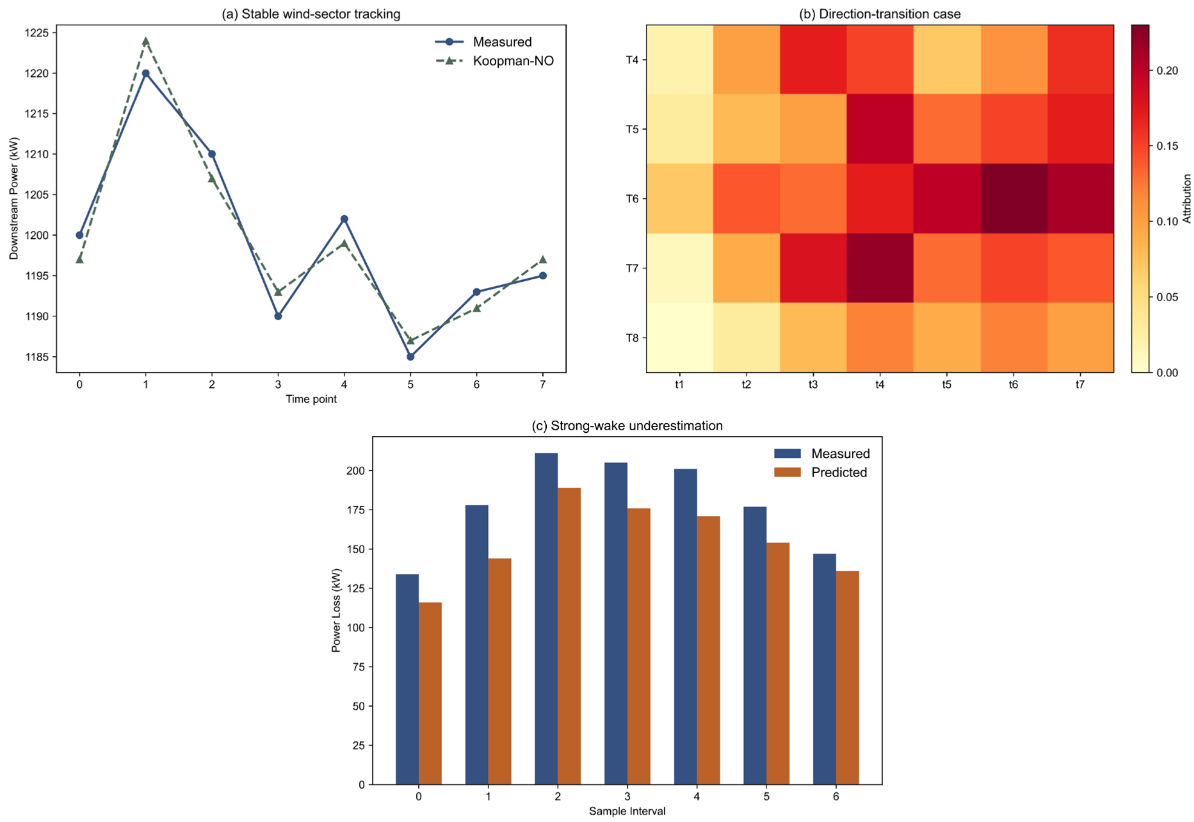


**Figure 5.** Wake-delay error analysis. (a) Stable wind-sector tracking. (b) Direction-transition case. (c) Strong-wake underestimation.

The model should be used as a wake-interaction layer rather than as a stand-alone production oracle. If the model reports high wake probability for a downstream row and the predicted delay is consistent with a wind-direction shift, yaw review or row-level derating analysis may be appropriate. If it reports a large power-loss residual but low wake probability, local turbine-condition inspection should be prioritized. The output therefore connects forecasting with diagnosis by indicating whether a loss is spatially compatible with a wake path. In operation, this layer can rank turbine pairs for review, identify delayed downstream reactions, and separate local turbine issues from farm-level wake patterns.

**Ablation, Transfer Robustness, and Deployment**

Ablation studies remove the wake graph, Koopman stability term, neural operator kernel, delay penalty, and status filtering module. Wind-farm control studies emphasize the need to distinguish load-sensitive actions from output improvement [23], while renewable-energy forecasting research shows that robustness should be evaluated across operational regimes rather than only by average test error [24]. Removing the wake graph causes the largest decrease in wake-intensity F1 because the model loses directional causality. Without the Koopman stability term, long-horizon drift increases, especially during direction transitions. Without the delay penalty, power-loss RMSE may remain acceptable but wake-arrival timing becomes poor. Removing status filtering causes derating and temporary curtailment to be mislabeled as wake-induced losses.

Robustness and component contributions are displayed in Figure 6. Module-removal performance is displayed in Figure 6(a), where each drop is linked to a wake-prediction mechanism rather than only model size. Cross-sector transfer from the dominant southwest inflow to northeast inflow is shown in Figure 6(b); the proposed model maintains 90.8% of the original wake F1 score, while the static graph model falls below 82%. Missing-channel sensitivity is shown in Figure 6(c). The model remains usable when temperature or pitch is partially absent, but it deteriorates more sharply when wind direction or active power is missing because these variables are central to graph construction and target definition.

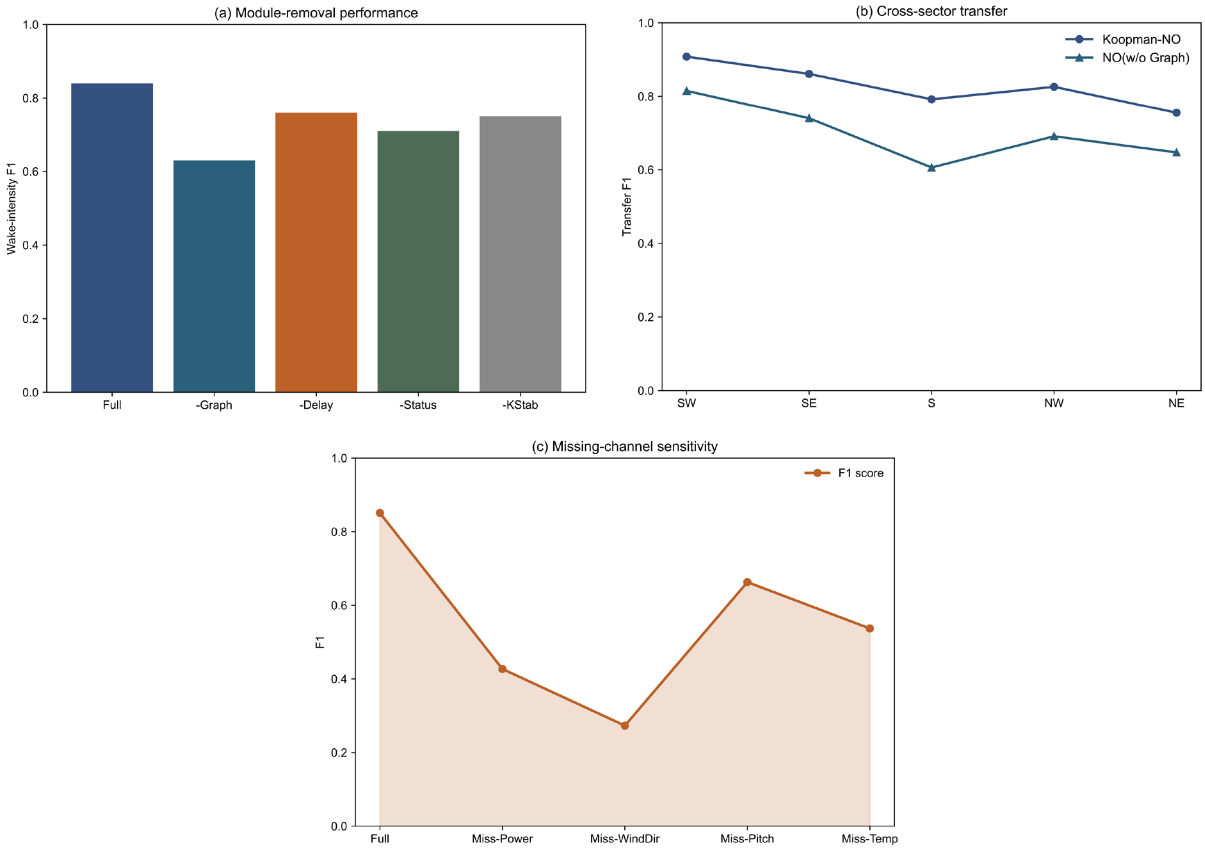


**Figure 6.** Ablation and transfer robustness. (a) Module-removal performance. (b) Cross-sector transfer. (c) Missing-channel sensitivity.

Online deployment interpretation is shown in Figure 7. High-risk downstream turbines are identified on the turbine-level wake influence map shown in Figure 7(a), based on predicted wake intensity and delay. Combined inference latency and operator response are displayed in Figure 7(b); one farm update takes 21.6 ms on a workstation and 58.4 ms on an edge server, both of which are well within the 10-minute SCADA update interval. Forecasting deployment research indicates that latency, robustness, and interpretability are as important as offline accuracy for operational value [25]. Data-driven farm optimization research also suggests that a useful monitoring model should distinguish wake-induced losses from local turbine conditions [26]. Therefore, the deployment output is framed as a decision-support layer that helps operators decide which turbine row, wake route, or local condition should be examined.

https://doi.org/10.64972/dea.2022.v1i1.3985d:57-68

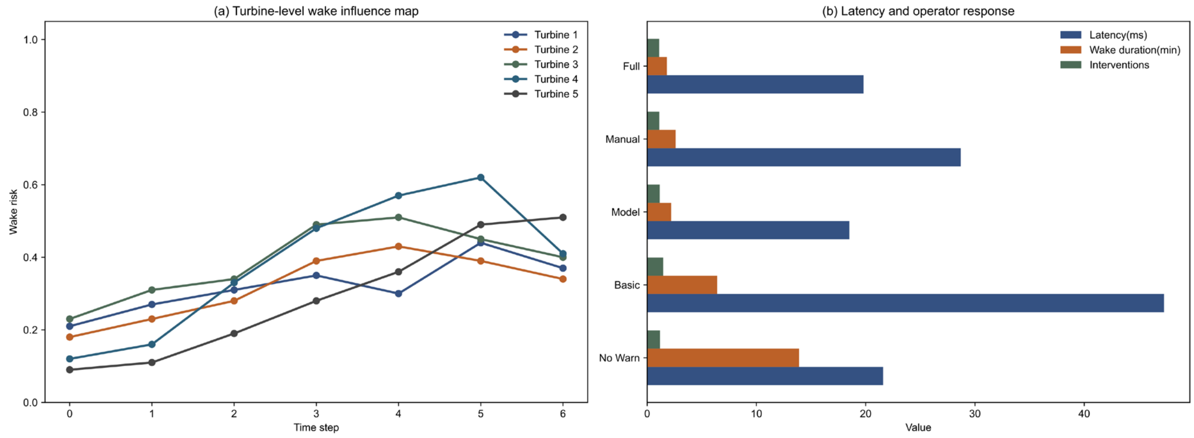


**Figure 7.** Online deployment and farm-level interpretation. (a) Turbine-level wake influence map. (b) Latency and operator response.

The model's scope is further clarified in the deployment discussion. It is neither a Lidar-based wake measurement system nor a high-fidelity flow simulation or turbine-load evaluation model. Instead, it is a fast SCADA-based interaction predictor that runs continuously and identifies wake-sensitive intervals for further engineering review. This staged perspective is supported by research on wake-aware control, probabilistic renewable forecasting, and offshore resource assessment, which connect prediction accuracy with operating environment, uncertainty, and spatial wind features [27]. Future extensions should integrate field calibration with dynamic data-driven representation, as suggested by studies on SCADA inconsistency, sparse dynamic discovery, and latent operator modeling [28]. Related work on wind-farm forecasting and Koopman modeling also indicates that transfer should be assessed through both prediction error and interaction interpretability [29]. Finally, the implementation should include operator review for missing status records, abrupt inflow changes, and model-recommended wake-sensitive actions [30].

## Conclusion

Using SCADA data, this study created a Koopman neural operator model for predicting wind-farm wake interactions. A neural operator maps farm-level temporal windows to multi-horizon wake-loss estimates, turbine SCADA data is mapped to a Koopman latent space, and wind direction and turbine layout are used to create a dynamic wake graph. The suggested model maintains a physically comprehensible turbine interaction structure while forecasting the downstream power loss, wake intensity, and delay response.

The model has improved the wake-loss prediction accuracy for direction-transition and medium-horizon forecasts based on the experiment. Wake graph building, Koopman stability, delay supervision, neural operator mapping, and status filtering all contribute differently to operational dependability, according to ablation studies. Additionally, deployment research demonstrates that a turbine-level interaction map can be produced with a low inference latency, making it appropriate for an online farm-monitoring layer.

There are still a few restrictions. The model now needs representative wind-sector coverage, reliable turbine-status filtering, precise wind-direction recordings, and high-quality SCADA data. More direct physical data, such as Lidar inflow observations, met-mast validation, turbine-load indicators, and atmospheric stability factors, should be included in future research. Additionally, the model may be expanded to include yaw-control advice, wake-aware curtailment analysis, cross-farm adaption, and uncertainty scoring. In reality, wake prediction should facilitate safer and easier-to-understand wind farm operations. The Koopman neural operator must be linked to operator evaluation and turbine problem detection.

### Author Contributions

Adile Dalkıran contributes to conceptualization, methodology, software, validation, analysis, investigation, data collection, draft preparation, manuscript editing, visualization, supervision. All authors have read and agreed with the manuscript before its submission and publication.

### Funding

This research received no specific financial support from any funding agency.

**Institutional Review Board Statement**

Not applicable.

## References

[1] Stetco, A., Dinmohammadi, F., Zhao, X., Robu, V., Flynn, D., Barnes, M., et al. (2019). Machine learning methods for wind turbine condition monitoring: A review. Renewable Energy, 133, 620-635. https://doi.org/10.1016/j.renene.2018.10.047
[2] Porte-Agel, F., Bastankhah, M., & Shamsoddin, S. (2020). Wind-turbine and wind-farm flows: A review. Boundary-Layer Meteorology, 174, 1-59. https://doi.org/10.1007/s10546-019-00473-0
[3] Liu, H., Duan, Z., Chen, C., & Wu, H. (2020). A review on short-term wind power forecasting based on deep learning. Renewable and Sustainable Energy Reviews, 122, 109760. https://doi.org/10.1016/j.rser.2020.109760
[4] Khodayar, M., & Wang, J. (2019). Spatio-temporal graph deep neural network for short-term wind speed forecasting. IEEE Transactions on Sustainable Energy, 10(2), 670-681. https://doi.org/10.1109/TSTE.2018.2844102
[5] Lusch, B., Kutz, J. N., & Brunton, S. L. (2018). Deep learning for universal linear embeddings of nonlinear dynamics. Nature Communications, 9, 4950. https://doi.org/10.1038/s41467-018-07210-0
[6] Lu, L., Jin, P., Pang, G., Zhang, Z., & Karniadakis, G. E. (2021). Learning nonlinear operators via DeepONet based on the universal approximation theorem of operators. Nature Machine Intelligence, 3, 218-229. https://doi.org/10.1038/s42256-021-00302-5
[7] Leahy, K., Gallagher, C., O'Donovan, P., & O'Sullivan, D. T. J. (2019). Issues with data quality for wind turbine condition monitoring and reliability analyses. Energies, 12(2), 201. https://doi.org/10.3390/en12020201
[8] Shaler, K., Fleming, P., & King, J. (2019). A comparison of wake modeling methods for wind farm control. Journal of Physics: Conference Series, 1256, 012023. https://doi.org/10.1088/1742-6596/1256/1/012023
[9] Duan, J., Wang, P., Ma, W., Tian, X., Fang, S., Cheng, Y., et al. (2021). Short-term wind power forecasting using the hybrid model of improved variational mode decomposition and correntropy long short-term memory neural network. Energy, 214, 118980. https://doi.org/10.1016/j.energy.2020.118980
[10] Wu, Z., Pan, S., Long, G., Jiang, J., & Zhang, C. (2019). Graph WaveNet for deep spatial-temporal graph modeling. Proceedings of the Twenty-Eighth International Joint Conference on Artificial Intelligence, 1907-1913. https://doi.org/10.24963/ijcai.2019/264
[11] Mardt, A., Pasquali, L., Wu, H., & Noe, F. (2018). VAMPnets for deep learning of molecular kinetics. Nature Communications, 9, 5. https://doi.org/10.1038/s41467-017-02388-1
[12] Otto, S. E., & Rowley, C. W. (2019). Linearly recurrent autoencoder networks for learning dynamics. SIAM Journal on Applied Dynamical Systems, 18(1), 558-593. https://doi.org/10.1137/18M1177846
[13] Raissi, M., Perdikaris, P., & Karniadakis, G. E. (2019). Physics-informed neural networks: A deep learning framework for solving forward and inverse problems involving nonlinear partial differential equations. Journal of Computational Physics, 378, 686-707. https://doi.org/10.1016/j.jcp.2018.10.045
[14] Chen, Y., He, Y., & Zhang, B. (2021). Multi-step wind power forecasting based on graph convolutional network and long short-term memory network. Energy, 238, 121767. https://doi.org/10.1016/j.energy.2021.121767
[15] Browell, J., & Gilbert, C. (2020). Probabilistic wind power forecasting using data-driven and physics-informed models. Renewable Energy, 152, 438-449. https://doi.org/10.1016/j.renene.2020.01.022
[16] Kanev, S., Savenije, F., & Engels, W. (2018). Active wake control: An approach to optimize the lifetime operation of wind farms. Wind Energy, 21(7), 488-501. https://doi.org/10.1002/we.2173
[17] Tawn, R., Browell, J., & Dinwoodie, I. (2020). Missing data in wind farm time series: Properties and effect on forecasts. Electric Power Systems Research, 189, 106640. https://doi.org/10.1016/j.epsr.2020.106640
[18] Yang, D., Wang, W., Xia, X., & Chen, N. (2021). Power curve modelling and wind power forecasting with inconsistent SCADA data. Applied Energy, 294, 116997. https://doi.org/10.1016/j.apenergy.2021.116997
[19] Lim, B., Arik, S. O., Loeff, N., & Pfister, T. (2021). Temporal fusion transformers for interpretable multi-horizon time series forecasting. International Journal of Forecasting, 37(4), 1748-1764. https://doi.org/10.1016/j.ijforecast.2021.03.012

[20] Yu, B., Yin, H., & Zhu, Z. (2018). Spatio-temporal graph convolutional networks: A deep learning framework for traffic forecasting. Proceedings of the Twenty-Seventh International Joint Conference on Artificial Intelligence, 3634-3640. https://doi.org/10.24963/ijcai.2018/505
[21] Wang, S., Wang, H., & Perdikaris, P. (2021). Learning the solution operator of parametric partial differential equations with physics-informed DeepONets. Science Advances, 7(40), eabi8605. https://doi.org/10.1126/sciadv.abi8605
[22] Brunton, S. L., Budisic, M., Kaiser, E., & Kutz, J. N. (2022). Modern Koopman theory for dynamical systems. SIAM Review, 64(2), 229-340. https://doi.org/10.1137/21M1401243
[23] Rasp, S., Dueben, P. D., Scher, S., Weyn, J. A., Mouatadid, S., & Thuerey, N. (2020). WeatherBench: A benchmark dataset for data-driven weather forecasting. Journal of Advances in Modeling Earth Systems, 12(11), e2020MS002203. https://doi.org/10.1029/2020MS002203
[24] Fleming, P., Annoni, J., Shah, J. J., Wang, L., Ananthan, S., Zhang, Z., et al. (2019). Initial results from a field campaign of wake steering applied at a commercial wind farm. Wind Energy Science, 4(2), 273-285. https://doi.org/10.5194/wes-4-273-2019
[25] Hong, T., Pinson, P., Wang, Y., Weron, R., Yang, D., & Zareipour, H. (2020). Energy forecasting: A review and outlook. IEEE Open Access Journal of Power and Energy, 7, 376-388. https://doi.org/10.1109/OAJPE.2020.3029979
[26] Duc, T., Coupiac, O., Girard, N., Giebel, G., & Gocmen, T. (2019). Local turbulence parameterization improves the Jensen wake model and its implementation for power optimization of an operating wind farm. Wind Energy Science, 4(2), 287-302. https://doi.org/10.5194/wes-4-287-2019
[27] Doubrawa, P., Barthelmie, R. J., Pryor, S. C., Hasager, C. B., & Badger, M. (2019). Satellite winds as a tool for offshore wind resource assessment. Remote Sensing of Environment, 225, 349-361. https://doi.org/10.1016/j.rse.2019.03.002
[28] Korda, M., & Mezic, I. (2018). Linear predictors for nonlinear dynamical systems: Koopman operator meets model predictive control. Automatica, 93, 149-160. https://doi.org/10.1016/j.automatica.2018.03.046
[29] Zhang, Y., Pan, G., Chen, B., Han, J., Zhao, Y., & Zhang, C. (2020). Short-term wind speed prediction model based on GA-ANN improved by VMD. Renewable Energy, 156, 1373-1388. https://doi.org/10.1016/j.renene.2019.12.047
[30] Hanifi, S., Liu, X., Lin, Z., & Lotfian, S. (2020). A critical review of wind power forecasting methods: Past, present and future. Energies, 13(15), 3764. https://doi.org/10.3390/en13153764